Proceedings of the 4th International Conference on Mechatronics and Smart Systems
DOI: 10.54254/2755-2721/2026.33313

From Pixels to Plumes: A Comparative Review of Spatial Resolution Effects in Methane Remote Sensing

Yixian Liu

Faculty of Arts and Social Sciences, University Malaya, Kuala Lumpur, Malaysia
23061733@siswa.um.edu.my

Abstract. Anthropogenic emission of methane is a very affordable way of mitigating the short-term climate change. Nevertheless, standard bottom-up emission inventories have a credibility gap because they do not capture intermittent super-emitters. Top-down observations may offer an option, as provided by satellites. Platforms with mixed-resolution, including Sentinel-5P, are, however, limited by the mixed-pixel dilution effect. Such an effect blurs concentration gradients and does not assign individual sources of emissions the correct attribution. This paper will provide a comparative analysis of Sentinel-5P and the next-generation high-resolution satellite, MethaneSAT. The paper examines the importance of spatial resolution in methane monitoring. The findings suggest that meter-scale resolution is an efficient approach to overcome pixel dilution and reconstruct the emission plumes physically. With high-resolution observations, a geospatial analysis framework involving spatial overlay and background removal can be applied. This integration no longer requires monitoring anomalies in a specific region, but on a per-facility basis. The paper also appraises existing shortcomings, such as sensitivity to weather conditions and wind prediction uncertainty. It also presents future directions, such as the use of AI to detect plumes and the creation of multi-layered satellite constellations.

Keywords: Methane remote sensing, spatial resolution effect, mixed-pixel dilution, plume reconstruction, point-source attribution

1. Introduction

When it comes to global climate change mitigation, lowering man-made methane (CH_4) emissions would be among the most cost-effective strategies for relatively short-term temperature stabilisation [1,2]. Nevertheless, national-statistics-based traditional bottom-up emission inventories lack significant credibility because they cannot capture transient super-emitters [3-5].

To overcome this drawback, top-down monitoring via satellites has emerged, with satellites such as Sentinel-5P enabling global-scale observations [6,7]. Practically, however, its coarse spatial resolution of about 5.5 km x 7 km causes significant mixing of oil and gas plant emissions and background signals [8]. The mixed-pixel dilution effect flattens concentration gradients and cannot accurately attribute a particular concentration to a concentration source.

To overcome this constraint, MethaneSAT, the next-generation high-resolution satellite, introduces a crucial change in spatial resolution [9]. It has a resolution of meters (around 100 m x

© 2026 The Authors. This is an open access article distributed under the terms of the Creative Commons Attribution License 4.0 (https://creativecommons.org/licenses/by/4.0/).

DOI: 10.54254/2755-2721/2026.33313

400 m) with a swath width of approximately 200 km. This advantage effectively reduces pixel dilution, enabling fixed detection and morphological reconstructions of large- and small-scale emission plumes.

In a spatial analysis context, high-resolution imagery can be strictly superimposed on the oil and gas infrastructure in vector format [6,10]. Such integration provides markedly better accuracy in point-source attribution. It supports a shift to satellite-based independent verification of methane regulation on a global scale, rather than merely coarse regional estimation.

This paper investigates the redefinition of spatial resolution that can transform methane monitoring by turning indistinct pixels into distinct emission plumes. It initially examines the mechanics of multi-scale remote sensing of the environment. It then discusses a spatial analytical model for background removal and plume reconstruction using high-resolution imagery. The analysis also assesses practical performance under normal conditions, such as in long-distance pipelines and dense production basins. Lastly, the paper discusses the existing technical constraints and prospects for multi-scale cooperative monitoring.

2. From physical detection to spatial attribution: the underlying logic of satellite-based methane monitoring

Satellite remote sensing of atmospheric methane concentrations relies on detecting a specific spectral absorption feature with sensors on board the satellites [7,11]. But converting this physical signal into accurate localisation of surface-emission sources is difficult. The major constraint is the variability in spatial resolution across sensor generations.

The second section examines the physical mechanisms underlying methane detection and describes how changes in spatial scale transform the theoretical framework of point-source attribution.

2.1. How satellites detect methane: spectral absorption and measurement principles

As a ray of solar radiation travels through the atmosphere and is reflected toward a satellite, methane molecules absorb it in the shortwave infrared (SWIR) range, especially at 1.6 um [11,12]. This radiative transfer is Beer-Lambert Law-based, which simplistically can be stated as:

$$I(\lambda) = I_0(\lambda)\, exp\left(-\int \sigma(\lambda, p, T)\, n(s)\, ds\right) \tag{1}$$

In this equation, I(λ) represents the spectral radiance received by the sensor. $I_0(\lambda)$ denotes the solar irradiance at the top of the atmosphere. Sigma is the absorption cross-section of methane molecules. n(s) refers to the number density of atmospheric methane molecules along the optical path.

By solving Equation (1) using inversion algorithms and incorporating atmospheric pressure and terrain data, the system ultimately derives the column-averaged dry-air mole fraction of methane (XCH_4).

$$XCH_4 = VCD(CH_4) / VCD(air) = \int n(CH_4)(z)dz / \int n(air)(z)dz \tag{2}$$

In practical terms, the satellite functions as a spaceborne high-spectral-resolution imaging device that measures methane concentration by detecting characteristic absorption features in reflected

DOI: 10.54254/2755-2721/2026.33313

sunlight [7]. The effective pixel size, or spatial resolution, however, is the basic determinant of the sensor's capacity to resolve small leakage strengths at the scale [6,13].

Table 1 illustrates that Sentinel-5P will be configured to map the whole world in a day, with the pixel size set to about 5.5 km by 7 km [7,8]. This pixel size is sufficient for capturing general background concentrations but is evidently insufficient to resolve individual industrial facilities. By comparison, at a meter-scale resolution (of the order of 100 m to 400 m), MethaneSAT has a swath width of roughly 200 km [9]. With this improvement, the sensor is much more sensitive to small emission sources.

Table 1. Comparison of core technical parameters between Sentinel-5P and MethaneSAT

Parameter	Sentinel-5P (TROPOMI)	MethaneSAT	Key Impact on Monitoring
Spatial Resolution	5.5 km × 7 km	~100 m × 400 m	Determines whether the mixed-pixel dilution effect can be effectively mitigated and background interference can be removed.
Swath Width	2600 km	~200 km	Determines the single-pass coverage capability for specific oil and gas basins or pipeline systems.
Precision	~10 ppb	~3 ppb	Determines whether small- to medium-intensity facility-level leaks can be detected.
Primary Mission	Global Mapping	Facility-scale Targeting	Determines whether the technology functions as a "survey" tool or a "precise verification" tool in emission mitigation.

2.2. Limitations of coarse resolution: mixed-pixel dilution and signal aliasing

In practice, the change in the column concentration of methane (released by a point-source) (ΔXCH_4) depends negatively on the size occupied by a satellite pixel [6,13]. The bigger the pixels, the greater the dilution of the localised high-concentration signals by the background atmosphere.

In the case of Sentinel-5P, a localised plume of cross-section a few tens of meters can be covered by a large pixel of up to 38.5 km² [8]. When this happens, the signal is highly averaged with the background and is hard to discern. In highly complex geological environments, e.g., the Yakeles gas field, Tarim Basin (Figure 1(a), both natural micro-seepage and anthropogenic emissions are heavily mixed within coarse pixels. This intermingling, called signal aliasing, makes interpretation even more difficult.

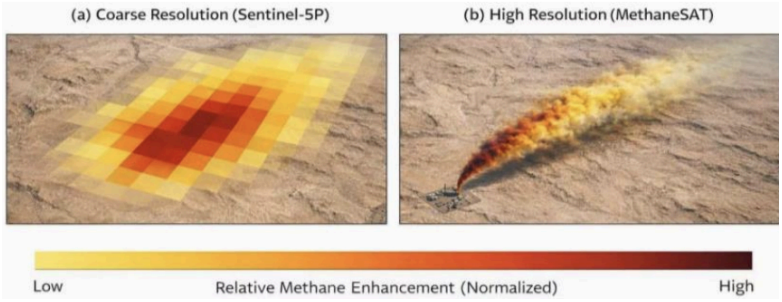


Figure 1. Comparison of mixed-pixel dilution effects under coarse resolution (Sentinel-5P) and high resolution (MethaneSAT)

The mixed-pixel dilution effect averages out the concentration gradients of leakage plumes. It does not permit them to be correctly attributed to any particular physical source, e.g. to particular wellheads [3,6].

DOI: 10.54254/2755-2721/2026.33313

In response to this shortcoming, MethaneSAT will use a much different spatial sampling approach [9]. Its pixel size, as shown in Figure 1, is reduced many times, thereby seriously impairing spatial averaging. This transformation of the scale maintains a high-concentration focus on the centre of emission sources and generates distinct spatial gradients in the image. Consequently, signal aliasing is effectively eliminated, and medium- to small-scale emission plumes can be visualised reliably.

2.3. Breaking the constraint with high resolution: GIS-based precise point-source attribution

High spatial resolution not only improves image clarity but also enables new approaches to spatial information analysis [6,10]. In the interest of obtaining proper point-source attribution in a challenging surface setup, the present methods would go beyond single spectral inversion and incorporate both spatial overlay and backtracking methodologies within a Geographic Information System (GIS) paradigm.

There are three major steps in the standard analytic workflow, depicted in Figure 2:

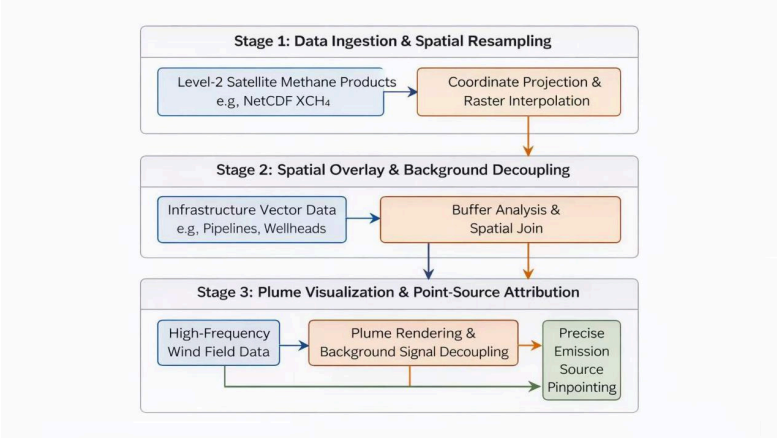


Figure 2. Spatial data processing workflow for methane point-source attribution based on GIS. To identify the source, the framework comprises three key steps: spatial resampling of Level-2 satellite data, spatial overlay with infrastructure vector data, and plume visualisation

3. Multi-scale monitoring performance in typical geographic settings

The enhancement of spatial resolution at the theoretical level is translated into a fundamentally different decision-support provision in the real-world methane mitigation area [6,9,14]. MethaneSAT and Sentinel-5P are characterised by obvious variations in work under difficult geographic conditions.

3.1. Distributed infrastructure across regions: detection of small leaks in long-distance pipelines

Here, leakage points are sparse and discontinuous in long-distance and cross-regional oil and gas pipeline networks, such as the West-East Gas Pipeline [4,15]. In this case, Sentinel-5P is capable of identifying methane anomalies in an area. Its rough pixels, however, are hundreds of kilometres long along the pipeline paths and merely point to a general alarm zone [8]. This constraint does not allow accurate localisation of individual emission points.

DOI: 10.54254/2755-2721/2026.33313

Conversely, MethaneSAT, with meter-scale resolution, can be closely compatible with pipeline vector networks [9]. In a GIS, a buffer analysis allows the merging of high-precision pipeline boundaries with the concentration rasters derived from MethaneSAT. The process eliminates the effects of background clutter on nearby land cover, such as farmland or wetlands. Consequently, point-level attribution of small sources of leakages is possible. This feature not only transforms monitoring into a form of blind inspection but also enables it to intervene with specific remote sensing coordinates.

3.2. Dense production facilities: independent verification at the facility level

In high-density fossil energy production areas, the granularity of emission inventory verification is constrained by spatial resolution. Han et al. (2024) [10] demonstrate that localised hotspots that are not identifiable using conventional inventories can be detected using high-resolution satellite observations.

Using Sentinel-5P in the above settings means that the waste gas emitted by other wells or gathering areas is highly mixed into a single pixel [8]. Such mixing does not allow attribution to individual sources.

MethaneSAT provides an independent verification method [9]. Recent work using facility-level satellite observations has further confirmed the feasibility of this approach [16,17]. In a GIS analytical environment, the loci of facilities may be spatially appended to high-frequency, high-resolution MethaneSAT imagery. This workflow helps to determine emissions of single facilities quickly. It can also support good geospatial evidence that can be used to implement emission-reduction policies [2,18,19].

In a bid to demonstrate the performance benefits of increased spatial resolution, Table 2 compares the attribution performance of Sentinel-5P and MethaneSAT in the following two typical industrial cases.

Table 2. Comparison of spatial attribution capabilities between Sentinel-5P and MethaneSAT in typical operational scenarios

Scenario	Infrastructure Features	S5P Capability	MethaneSAT Capability
Pipelines	Highly dispersed, linear distribution with complex background conditions.	Only capable of triggering large-scale regional anomaly alerts along pipeline corridors.	With buffer analysis, precise localisation of small leaks at specific valve stations or pipeline segments is achievable.
Basins	High facility density with point clustering and severe signal mixing.	Signals from multiple adjacent wells are strongly mixed within a single large pixel, preventing point-source attribution.	Background concentrations can be removed, enabling independent verification and inventory validation of individual facilities that are leaking.

4. Conclusion

This paper compares the spatial performance of a survey-based satellite, Sentinel-5P, and next-generation MethaneSAT in methane remote sensing. The findings demonstrate that MethaneSAT, a meter-scale resolution with a broad swath width, can successfully overcome the mixed-pixel dilution effect, which is restrictive in traditional systems.

Reconstruction at the plume level, rather than pixel-based signals, eliminates background interference and properly attributes individual oil and gas facilities. This development transforms the

DOI: 10.54254/2755-2721/2026.33313

paradigm of monitoring to comprise regional anomaly monitoring to facility monitoring. It further provides strong spatial evidence to close the credibility gap in conventional bottom-up emission inventories. Consequently, international governance of methane is shifting towards an autonomous verification system based on satellite monitoring.

Notwithstanding these developments, the high-resolution satellite-based verification system currently has various technical shortcomings. Remote sensing in the shortwave infrared (SWIR) is incredibly sensitive to the atmospheric effects. Surface reflectance, aerosol loading, and cloud cover can decrease data availability. Moreover, near-surface wind-field measurements are essential for converting plume morphology into precise estimates of emissions flux. Systematic errors in estimating the flux can arise from uncertainty in transient wind conditions [20].

The other obstacle is the multi-source integrations. Integrating multi-scale and multi-temporal satellite data into a GIS format is challenging. The process of algorithmic harmonisation across heterogeneous datasets also needs further development.

Further studies should aim to develop a multi-scale, collaborative system to monitor methane. Developing automated methods for plume detection using artificial intelligence and computer vision [21,22] to work with multiple high-resolution data volumes is a priority.

The next focus is on the Multi-level satellite constellations, comprising Sentinel-5P to conduct screening at large scales [23], MethaneSat to check, and GHGSat [24] to track specific behaviours. When linked to three-dimensional dynamic wind-field models, such as those developed by Meteorological Agencies, this will enhance attribution accuracy [25].

Further development of such technologies will be needed to support the introduction of the Global Methane Pledge and increase the visibility of worldwide emission-reduction endeavours.

References

[1] UNEP & CCAC. (2021). Global Methane Assessment: Benefits and Costs of Mitigating Methane Emissions. United Nations Environment Programme, Nairobi.

[2] IEA. (2024). Global Methane Tracker 2024. International Energy Agency, Paris. https: //www.iea.org/reports/global-methane-tracker-2024

[3] Cusworth, D. H., Jacob, D. J., Sheng, J.-X., Benmergui, J., Turner, A. J., Brandman, J., White, L., & Randles, C. A. (2018). Detecting high-emitting methane sources in oil/gas fields using satellite observations. Atmospheric Chemistry and Physics, 18, 16885–16896. https: //doi.org/10.5194/acp-18-16885-2018

[4] Pandey, S., Gautam, R., Houweling, S., Denier van der Gon, H., Sadavarte, P., Borsdorff, T., Hasekamp, O., Landgraf, J., Tol, P., van Kempen, T., Hoogeveen, R., van Hees, R., Hamburg, S. P., Maasakkers, J. D., & Aben, I. (2019). Satellite observations reveal extreme methane leakage from a natural gas well blowout. Proceedings of the National Academy of Sciences, 116(52), 26376–26381. https: //doi.org/10.1073/pnas.1908712116

[5] Lauvaux, T., Giron, C., Mazzolini, M., d'Aspremont, A., Duren, R., Cusworth, D., Shindell, D., & Ciais, P. (2022). Global assessment of oil and gas methane ultra-emitters. Science, 375, 557–561. https: //doi.org/10.1126/science.abj4351

[6] Jacob, D. J., Varon, D. J., Cusworth, D. H., Dennison, P. E., Frankenberg, C., Gautam, R., Guanter, L., Kelley, J., McKeever, J., Ott, L. E., Poulter, B., Qu, Z., Thorpe, A. K., Worden, J. R., & Duren, R. M. (2022). Quantifying methane emissions from global to point-source scales using satellite observations of atmospheric methane. Atmospheric Chemistry and Physics, 22, 9617–9646. https: //doi.org/10.5194/acp-22-9617-2022

[7] Hu, H., Hasekamp, O., Butz, A., Galli, A., Landgraf, J., Aan de Brugh, J., Borsdorff, T., Scheepmaker, R., & Aben, I. (2016). The operational methane retrieval algorithm for TROPOMI. Atmospheric Measurement Techniques, 9, 5423–5440. https: //doi.org/10.5194/amt-9-5423-2016

[8] Lorente, A., Borsdorff, T., Butz, A., Hasekamp, O., aan de Brugh, J., Schneider, A., Wu, L., Hase, F., Kivi, R., Wunch, D., Pollard, D. F., Shiomi, K., Deutscher, N. M., Velazco, V. A., Landgraf, J., & Aben, I. (2021). Methane retrieved from TROPOMI: improvement of the data product and validation of the first 2 years of measurements. Atmospheric Measurement Techniques, 14, 665–684. https: //doi.org/10.5194/amt-14-665-2021

DOI: 10.54254/2755-2721/2026.33313

[9] Staebell, A., Sun, K., Varon, D. J., Maasakkers, J. D., Turner, A. J., Chance, K., & Jacob, D. J. (2021). Spectral design of the MethaneSAT instrument. Atmospheric Measurement Techniques, 14, 3737–3753. https: //doi.org/10.5194/amt-14-3737-2021

[10] Han, G., Pei, Z., Shi, T., Mao, H., Li, S., Mao, F., Ma, X., Zhang, X., & Gong, W. (2024). Unveiling unprecedented methane hotspots in China's leading coal production hub: A satellite mapping revelation. Geophysical Research Letters, 51, e2024GL109065. https: //doi.org/10.1029/2024GL109065

[11] Schneising, O., Buchwitz, M., Reuter, M., Vanselow, S., Bovensmann, H., & Burrows, J. P. (2020). Remote sensing of methane leakage from natural gas and petroleum systems revisited. Atmospheric Chemistry and Physics, 20, 9169–9182. https: //doi.org/10.5194/acp-20-9169-2020

[12] Schneising, O., Buchwitz, M., Hachmeister, J., Vanselow, S., Reuter, M., Buschmann, M., Bovensmann, H., & Burrows, J. P. (2023). Advances in retrieving XCH_4 and XCO from Sentinel-5 Precursor: improvements in the scientific TROPOMI/WFMD algorithm. Atmospheric Measurement Techniques, 16, 669–694. https: //doi.org/10.5194/amt-16-669-2023

[13] Sherwin, E. D., Rutherford, J. S., Chen, Y., Aminfard, S., Kort, E. A., Jackson, R. B., & Brandt, A. R. (2023). Single-blind validation of space-based point-source detection and quantification of onshore methane emissions. Scientific Reports, 13, 3836. https: //doi.org/10.1038/s41598-023-30761-2

[14] Duren, R. M., Thorpe, A. K., Foster, K. T., Rafiq, T., Hopkins, F. M., Ber, V., Mber, S., Prasad, K., & Miller, C. E. (2019). California's methane super-emitters. Nature, 575, 180–184. https: //doi.org/10.1038/s41586-019-1720-3

[15] Dogniaux, M., Maasakkers, J. D., Girard, M., et al. (2025). Global satellite survey reveals uncertainty in landfill methane emissions. Nature, 647, 397–402. https: //doi.org/10.1038/s41586-025-09683-8

[16] Jervis, D., Durak, B. O. A., Gains, D., Ramier, A., McCloskey, S., & Sloan, J. J. (2025). Global energy-sector methane emissions estimated using facility-level satellite observations. Science, 386, eadv3183. https: //doi.org/10.1126/science.adv3183

[17] Guanter, L., Roger, J., Warren, J., Sargent, M., Zhang, Z., Roche, S., Miller, C. C., Steiner, M., Hadfield, H., Omara, M., Williams, J., MacKay, K., Franklin, J. E., Luo, B., Wofsy, S. C., Hamburg, S. P., & Gautam, R. (2026). Surveying methane point-source super-emissions across oil and gas basins with MethaneSAT. Atmospheric Chemistry and Physics, 26, 2941–2963. https: //doi.org/10.5194/acp-26-2941-2026

[18] Mohammadimanesh, F., Mahdianpari, M., Radman, A., Varon, D., Hemati, M., & Marjani, M. (2025). Advancements in satellite-based methane point source monitoring: A systematic review. ISPRS Journal of Photogrammetry and Remote Sensing, 224, 94–112. https: //doi.org/10.1016/j.isprsjprs.2025.03.020

[19] Guanter, L., Irakulis-Loitxate, I., Gorroño, J., Sánchez-García, E., Cusworth, D. H., Varon, D. J., Cogliati, S., & Colombo, R. (2025). Sectoral contributions of high-emitting methane point sources from major US onshore oil and gas producing basins using airborne measurements from MethaneAIR. Atmospheric Chemistry and Physics, 25, 10661–10681. https: //doi.org/10.5194/acp-25-10661-2025

[20] Varon, D. J., Jacob, D. J., McKeever, J., Jervis, D., Durak, B. O. A., Xia, Y., & Huang, Y. (2018). Quantifying methane point sources from fine-scale satellite observations of atmospheric methane plumes. Atmospheric Measurement Techniques, 11, 5673–5686. https: //doi.org/10.5194/amt-11-5673-2018

[21] Rouet-Leduc, B., & Hulbert, C. (2024). Automatic detection of methane emissions in multispectral satellite imagery using a vision transformer. Nature Communications, 15, 3801. https: //doi.org/10.1038/s41467-024-47754-y

[22] Schuit, B. J., Maasakkers, J. D., Bijber, P., Mahber, G., Bremser, A. B., Hber, N. S., Lorber, J. C., Irakulis-Loitxate, I., Gorroño, J., Guanter, L., Cusworth, D. H., Varon, D. J., Sherwin, E. D., & Aben, I. (2023). Automated detection and monitoring of methane super-emitters using satellite data. Atmospheric Chemistry and Physics, 23, 9071–9098. https: //doi.org/10.5194/acp-23-9071-2023

[23] Irakulis-Loitxate, I., Guanter, L., Maasakkers, J. D., Zavala-Araiza, D., & Aben, I. (2022). Satellites detect abatable super-emissions in one of the world's largest methane hotspot regions. Environmental Science & Technology, 56(4), 2143–2152. https: //doi.org/10.1021/acs.est.1c04873

[24] Jervis, D., McKeever, J., Durak, B. O. A., Sloan, J. J., Gains, D., Varon, D. J., Ramber, A., Struber, M., Rber, E., & Pacheco, M. (2021). The GHGSat-D imaging spectrometer. Atmospheric Measurement Techniques, 14, 2127–2140. https: //doi.org/10.5194/amt-14-2127-2021

[25] Cusworth, D. H., Duren, R. M., & Thorpe, A. K. (2021). Multisatellite imaging of a gas well blowout enables quantification of total methane emissions. Geophysical Research Letters, 48, e2020GL090864. https: //doi.org/10.1029/2020GL090864